

Epitaxial growth of lead zirconium titanate thin films on Ag buffered Si substrates using rf sputtering

Chun Wang,^{a)} David E. Laughlin, and Mark H. Kryder

Department of Electrical and Computer Engineering, Data Storage Systems Center, Carnegie Mellon University, Pittsburgh, Pennsylvania 15213

(Received 7 February 2007; accepted 25 March 2007; published online 23 April 2007)

Epitaxial lead zirconium titanate (PZT) (001) thin films with a Pt bottom electrode were deposited by rf sputtering onto Si(001) single crystal substrates with a Ag buffer layer. Both PZT(20/80) and PZT(53/47) samples were shown to consist of a single perovskite phase and to have the (001) orientation. The orientation relationship was determined to be PZT(001)[110]||Pt(001)[110]||Ag(001)[110]||Si(001)[110]. The microstructure of the multilayer was studied using transmission electron microscopy (TEM). The electron diffraction pattern confirmed the epitaxial relationship between each layer. The measured remanent polarization P_r and coercive field E_c of the PZT(20/80) thin film were $26 \mu\text{C}/\text{cm}^2$ and $110 \text{ kV}/\text{cm}$, respectively. For PZT(53/47), P_r was $10 \mu\text{C}/\text{cm}^2$ and E_c was $80 \text{ kV}/\text{cm}$. © 2007 American Institute of Physics. [DOI: 10.1063/1.2731515]

The ferroelectric material lead zirconium titanate [Pb(Zr,Ti)O₃ or PZT] is a promising medium for scanning probe microscopy-based high density data storage.¹ Compared with ferromagnetic materials, ferroelectric materials have the advantages of narrower domain width, fast switching of polarization, and electrical operation. For probe storage media, large remanent polarization and uniform properties are desirable. Compared to other ferroelectric materials such as BaTiO₃, PZT has stronger polarization and lower processing temperature. Therefore, epitaxially grown PZT thin films with controlled orientation are of interest for probe storage applications. Though researchers have already obtained good epitaxial PZT thin films on some single crystal substrates such as SrTiO₃, MgO, and LaAlO₃ using different deposition methods (sputtering, pulsed laser deposition, and metal-organic chemical-vapor deposition),²⁻⁴ fabrication on silicon is preferred for industrial applications, because it is a much cheaper substrate and also provides the promise that it can be integrated with a complementary metal-oxide semiconductor process. Thus, the epitaxial growth of ferroelectric thin films on Si using rf sputtering is a goal we want to reach. Platinum (Pt) is widely used as a bottom electrode material for ferroelectric thin film capacitors because of its good electrical conductivity and chemical stability. However, Pt films grown on titanium buffered Si(001) substrates are polycrystalline with the (111) orientation.⁵ In order to grow epitaxial Pt thin films, suitable buffer layers with good diffusion barrier properties and epitaxy with Si need to be used.

In this work, we investigated the feasibility of using Ag as a buffer layer for epitaxial growth of PZT films on Si(100) substrates. Ag is easily grown epitaxially on HF-etched Si(001) with cube-on-cube orientation relationship, though the lattice mismatch between Ag (fcc, $a=4.09 \text{ \AA}$) and Si (diamond cubic, $a=5.43 \text{ \AA}$) is about 24.7%.^{6,7} This is explained by the domain matching epitaxial model in which four planes of Ag match three planes of Si very well. The lattice mismatch between Pt (fcc, $a=3.92 \text{ \AA}$) and Ag is about 4.15%, while PZT(53/47) (rhombohedral, $a=4.07 \text{ \AA}$,

$c=4.15 \text{ \AA}$) has mismatch of 3.8% with respect to Pt. The schematic plot of the relative orientation is shown in Fig. 1.

Sputtering was used to deposit these epitaxial films on Si substrates in this work. First, a HF-cleaned Si substrate was placed into a Leybold-Heraeus Z-400 sputtering system. The base pressure was about 6×10^{-7} Torr. Pt and Ag thin films were then deposited at $300 \text{ }^\circ\text{C}$ sequentially by rf diode sputtering. The Ar sputtering gas pressure was fixed at 10 mTorr, and the sputtering power density was about $2.3 \text{ W}/\text{cm}^2$. The thickness of Ag and Pt were about 100 and 50 nm, respec-

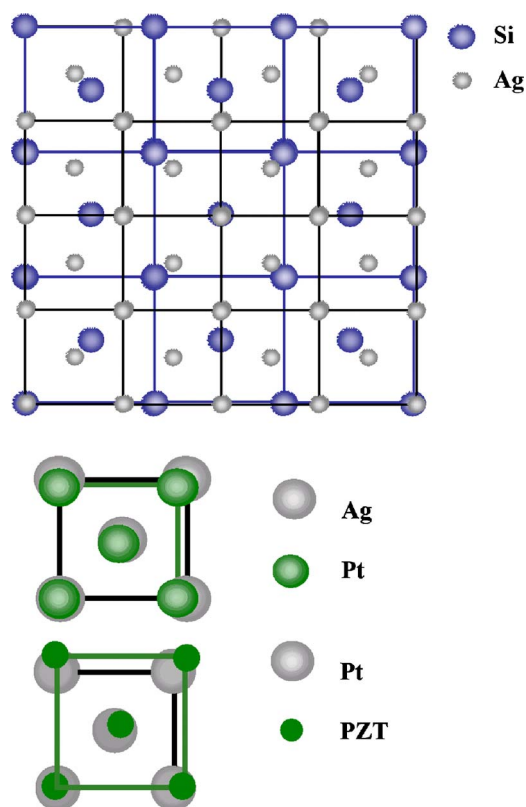


FIG. 1. (Color online) Orientation relationships between Si(001)/Ag(001), Ag(001)/Pt(001), and Pt(001)/PZT(001) planes.

^{a)}Electronic mail: chunw@andrew.cmu.edu

tively. During the experiment, it was found that the hydrogen terminated Si substrates oxidized very slowly in air, so that epitaxial Ag could still be obtained on Si that was cleaned 1 day before. After the Pt and Ag layers were deposited on the Si and cooled down to room temperature, the sample was transferred to a Lesker sputtering system with a 2 in. PZT composite target installed. Both PZT(20/80) and PZT(53/47), 140 and 160 nm, respectively, were sputtered in 5 mT Ar at room temperature with a power density of 2.5 W/cm². The as-deposited films were amorphous and transformed into the perovskite phase after annealing in O₂ at 700 °C for 1 min using rapid thermal annealing. Pt (100 nm), for the top electrode, was sputtered at room temperature through a shadow mask with different diameters of 0.01, 0.02, and 0.03 in. The orientation and microstructure of the PZT samples were determined by a Philips x-ray diffractometer with Cu K α radiation and a JEM 2000 EX II transmission electron microscope (TEM). The surface roughness of the PZT films was studied by atomic force microscopy (AFM).

The x-ray diffraction (XRD) θ -2 θ spectrum for the sample PZT(53/47)/Pt/Ag/Si is shown in Fig. 2(a). Only strong (002) diffraction peaks are seen for Ag and Pt films. No Ag(111) or Pt (111) peaks were observed. The Φ scan of (110) planes of Si, Ag, and Pt is shown in Fig. 2(b). The four sharp peaks of the different films at the same position indicate cube-on-cube epitaxial relations between each layer. The PZT layer is a single phase perovskite with the (001) orientation. The PZT(002) peak was hidden by Ag(002) and Pt(002) peaks because of the strong intensity of the metal peaks. The Φ scans of (110) planes were performed for Pt and PZT layers as shown in Fig. 2(c). The fourfold symmetry peaks indicate that the PZT layer is also highly oriented in the plane and has good cube-on-cube alignment with Pt. The XRD θ -2 θ spectrum of PZT(20/80)/Pt/Ag/Si is shown in Fig. 2(d). A strong PZT(001) peak was obtained on the epitaxial Pt layer. The Φ scans of (110) planes for the Pt and PZT layers are shown in Fig. 2(e). The fourfold symmetry peaks indicate that PZT(20/80) also grows epitaxially on Si substrates with a cube-on-cube relationship. X-ray rocking curve measurements were performed to evaluate the crystalline quality of the films. The full width at half maximum (FWHM) of the rocking curve for PZT(53/47) (001) is 2.5°, FWHM of PZT(20/80) (001) is 3.8°, FWHM of Pt(002) is 1.08°, and FWHM of Ag(002) is 0.95°. The surface roughness of the PZT films was studied by AFM. The best root-mean-square roughness obtained for Ag was 2 nm, for Pt was 1.5 nm, and for PZT was 0.9 nm before annealing and 2 nm after annealing. The increase of roughness of PZT films was caused by the formation of crystal grains.

Plane-view and cross-sectional TEM specimens were prepared using a standard preparation technique involving mechanical thinning, dimpling, and Ar ion milling. Figures 3(a) and 3(b) show a plane-view TEM image and a selected aperture diffraction (SAD) pattern of the PZT(53/47) samples. The plane-view TEM image shows that low angle grain boundaries exist in the PZT(53/47) films with a large distribution of grain sizes from 300 to 700 nm. The SAD pattern confirms that the PZT film was a (001)-oriented single crystal. Figures 3(c)–3(e) show a cross-sectional TEM image and SAD patterns of the PZT(20/80)/Pt/Ag/Si film. No oxide layer was observed

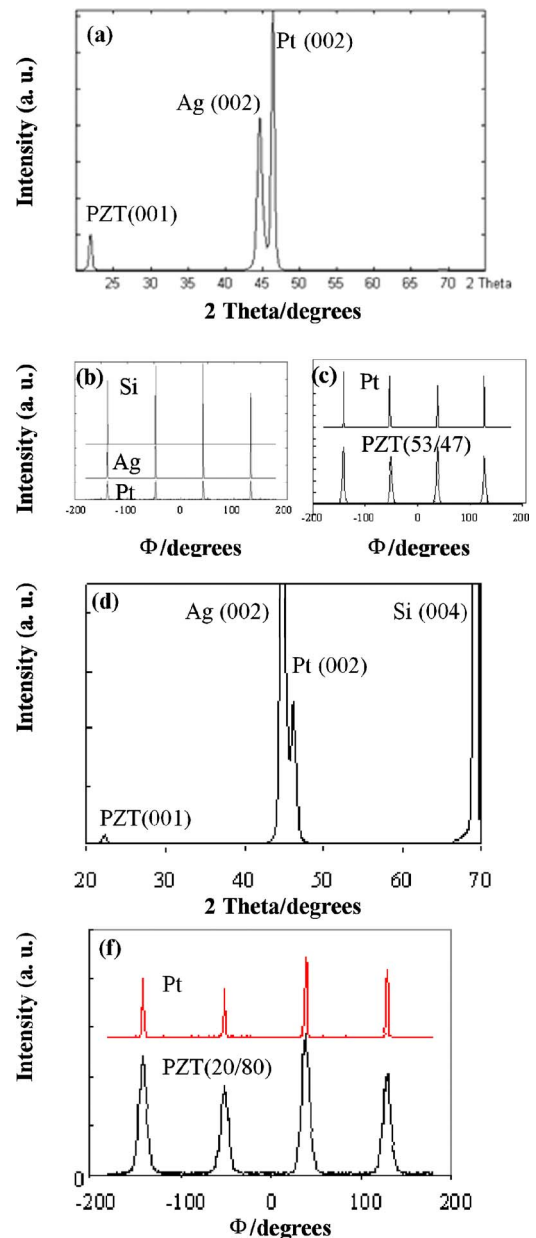


FIG. 2. (Color online) (a) XRD spectra of PZT(53/47)/Pt/Ag/HF–Si films. (b) Φ scans of (110) planes of Pt, Ag, and Si layers. (c) Φ scans of (110) planes of PZT(53/47) and Pt layers. (d) XRD spectra of PZT(20/80)/Pt/Ag/HF–Si films. (e) Φ scans of (110) planes of PZT(20/80) and Pt layers.

between Ag and Si. The surface smoothness of the Si substrate was disturbed in some areas due to the HF etching. The interface between Si and Ag was improved when shorter etching time was used. The SAD patterns were taken along the Si[110] and PZT[110] zone axis. Figures 3(d) and 3(e) display the SAD pattern of the Pt/Ag/Si structure and the SAD pattern of the PZT layer, respectively. The alignment of diffraction spots in three directions confirms the epitaxial relation between the various layers.

The P - E hysteresis loop was measured by a Sawyer-Tower circuit.⁸ The P - E hysteresis loops are shown in Figs. 4(a) and 4(b). The measured remanent polarization P_r and coercive field E_c of the PZT(20/80) thin film were 26 $\mu\text{C}/\text{cm}^2$ and 110 kV/cm. For PZT(53/47), P_r was 10 $\mu\text{C}/\text{cm}^2$ and E_c was 80 kV/cm. The leakage current densities for both PZT(20/80) and PZT(53/47) were around

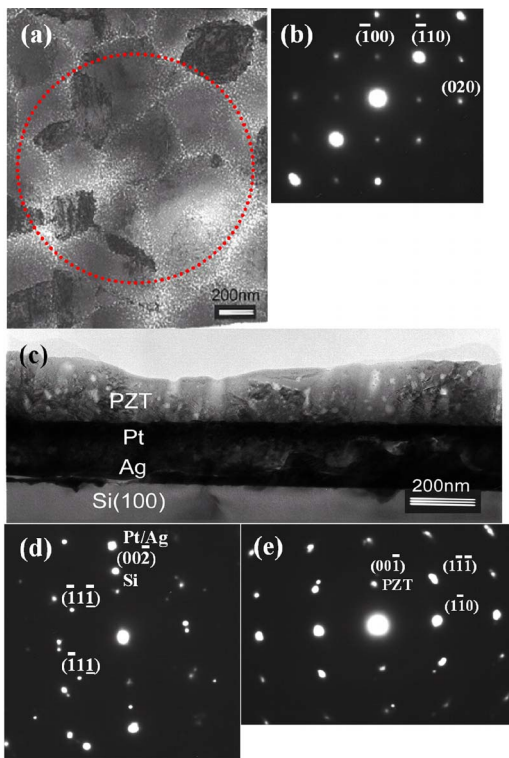


FIG. 3. (Color online) (a) Plane-view TEM image of the sample PZT(53/47)/Pt/Ag/Si. (b) Selected electron diffraction pattern of the PZT(53/47) film along the [001] zone axis. (c) Cross-sectional TEM image of the PZT(20/80)/Pt/Ag/Si sample. (d) Selected electron diffraction pattern of the Pt/Ag/Si structure along the S[110] zone axis. (e) Selected electron diffraction pattern of the PZT(20/80) layer along the PZT[110] zone axis.

2.4×10^{-7} A/cm² at 5 V. The PZT(20/80) sample shows stronger remanent polarization than the PZT(53/47) sample because the polar axis for PZT(20/80) is along the [001] direction while that of PZT(53/47) is along the [111] direction. Since both films are (001) oriented, for PZT(53/47), the measured polarization component along the [001] direction will be a factor of $1/\sqrt{3}$ of the polarization along the [111] direction. As expected, the hysteresis loop is more square for PZT(20/80) than PZT(53/47), because the voltage was applied along the polar axis of PZT(20/80)(001) while it was applied at an angle relative to [111] polar axis of PZT(53/47) sample. However, the epitaxial PZT(20/80) films still show lower polarization values than the PZT films on oxide single crystal substrates, because Si substrates apply a tensile stress to the PZT films during the cooling process due to different thermal expansion coefficients between the substrates and the films.⁹ The tensile stress causes “*a*” domains (polar axis in plane) to form, which reduces the total remanent polarization value along the out-of-plane direction.

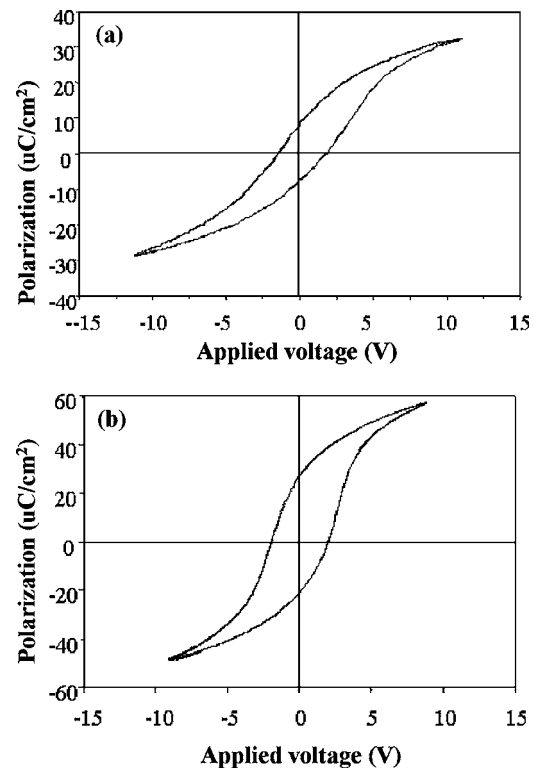


FIG. 4. *P-E* hysteresis loops of PZT capacitors using Pt top electrodes; (a) PZT(53/47) and (b) PZT(20/80).

In summary, we have successfully deposited epitaxial (001)-oriented PZT(20/80) and PZT(53/47) thin films on HF-etched Si(001) substrates with Ag templates by rf sputtering. The epitaxial orientation relationship of the various layers was cube on cube without relative rotation. The PZT(20/80) samples show a remanent polarization of $26 \mu\text{C}/\text{cm}^2$ and a coercive field of 110 kV/cm. The PZT(53/47) films show reasonable electrical properties with a remanent polarization of $10 \mu\text{C}/\text{cm}^2$ and a coercive field of 80 kV/cm. Therefore, integration of epitaxial PZT films with Si could be achieved using a single buffer layer of Ag.

¹Y. Cho, K. Fujimoto, Y. Hiranaga, Y. Wagatsuma, A. Onoe, K. Terabe, and K. Kitamura, *Nanotechnology* **14**, 637 (2003).

²L. Roytburd, S. P. Alpay, L. A. Bendersky, V. Nagarajan, and R. Ramesh, *J. Appl. Phys.* **89**, 553 (2001).

³C. B. Eom, R. B. Van Dover, Julia M. Phillips, D. J. Werder, J. H. Marshall, C. H. Chen, R. J. Cava, R. M. Fleming, and D. K. Fork, *Appl. Phys. Lett.* **63**, 2570 (1993).

⁴Junichi Ishida, Takatoshi Yamada, Atsuhito Sawabe, Kumi Okuwada, and Keisuke Saito, *Appl. Phys. Lett.* **80**, 467 (2002).

⁵C. Millon, C. Malhaire, C. Dubois, and D. Barbier, *Mater. Sci. Semicond. Process.* **5**, 243 (2002).

⁶W. Yang and D. N. Lambeth, *J. Appl. Phys.* **81**, 4370 (1997).

⁷T. Zheleva, K. Jagannadham, and J. Narayan, *J. Appl. Phys.* **75**, 860 (1994).

⁸C. B. Sawyer and C. H. Tower, *Phys. Rev.* **35**, 269 (1930).

⁹H. Morioka, G. Asano, T. Oikawa, H. Funakubo, and K. Saito, *Appl. Phys. Lett.* **82**, 4761 (2003).